Journal of Electronics and Electrical Engineering
https://ojs.wiserpub.com/index.php/JEEE

Research Article

17 Level Hybrid Diode Clamped Inverter with Reduced Number of Components

Mohammed Alsumady[1*], Ibrahim Jaber[2], Khalid Nusserat[3]

[1] Department of Electronic Engineering, Yarmouk University, Irbid, Jordan
[2] Analog and Mixed Signal IC Layout Engineer, Golden Electronics, Amman, Jordan
[3] Department of Computer Engineering, Yarmouk University, Irbid, Jordan
[*] Correspondence: alsumady@yu.edu.jo

Received: 24 June 2023; **Revised:** 10 September 2023; **Accepted:** 14 September 2023; **Published:** 26 September 2023

Abstract: Multilevel inverters (MLIs) have recently gained increasing interest in medium- to high-power applications. The main challenge with various MLI topologies is their requirement for a large number of switching devices and DC voltage sources while generating a limited number of voltage levels, resulting in bulky, costly inverters with high output voltage/current Total Harmonic Distortion (THD). This paper proposes a novel asymmetrical 17-level MLI design that utilizes only two DC voltage sources and a reduced number of switches. This is achieved by combining a voltage summing and subtracting circuit with a modified Diode-Clamped MLI (DC-MLI), which divides the voltage by two, thereby generating more voltage levels. The Nearest Level Control (NLC) method is used to generate switching signals at a fundamental frequency of 50 Hz. The design is tested and simulated using MATLAB/Simulink, with the output voltage THD maintained at approximately 5.7%. The obtained results are compared with other recent 17-level topologies, demonstrating a notable improvement.

***Keywords*:** multilevel inverter, Nearest Level Control (NLC), neutral point clamped, simulink, switching devices, Total Harmonic Distortion (THD)

1. Introduction

The main two types of inverters are Pulse Width Modulation (PWM) inverters and Multilevel Inverters, MLI topologies include flying capacitor (FC), diode clamped and Cascaded H-Bridge (CHB) multilevel inverters [1]. Some of the advantages of MLIs are having lower Total Harmonic Distortion, higher output power and no need for output filtering [2, 3]. Due to these advantages, MLIs caught the attention of researchers lately and they are used widely in photovoltaic (PV) systems [4], Electric Vehicles (EVs) [5], and Uninterruptable Power Supplies (UPS) [6–8].

One problem in the various designed MLIs is the large number of switches and DC sources which increases the cost and the size of the inverter [9]. Another problem arises when the number of levels is small; This increases the THD and causes a large *dv*/*dt* stress over the switching devices [10, 11].

In [11], a seven level PWM inverter utilizing three series connected capacitors was designed; The three series capacitors divide the input voltage into three equal quantities which can be used to generate the seven voltage levels. One of its advantages is the need for one voltage source and seven switches only. However, the three capacitors need careful

DOI: https://doi.org/10.37256/jeee.2220233266

balancing to ensure right operation of the inverter, and it generates only seven levels. Paper [12] introduces a modified five level (DC-MLI), the design was achieved by adding two switches to the traditional three level DC-MLI, which provided the ability to utilize the voltage of the source in addition to the DC bus capacitors voltages, the design uses a single source and six unidirectional switches. However, the number of levels is considered to be low. [13] introduced an asymmetrical 17-level inverter using 11 unidirectional switches, which is a good improvement. But it requires 3 DC sources that increase the size and the cost of the inverter.

In this paper the proposed design reduces the number of components, introduces a comparable low-cost low complexity inverter with high number of levels and an acceptable voltage THD.

2. Proposed design

The general idea of the proposed design is to combine two circuits, one of which adds and subtracts the two input voltages, whereas the other divide the DC voltage by two, this way more levels can be generated from a given number of sources [14].

2.1 *Circuit description*

The circuit design is shown in Figure 1, it consists of 12 switches SW1-12, two DC sources V_A and V_B, two diodes and two capacitors. The best ratio for the DC sources, V_B:V_A was found to be 1:5 by using a designed code.

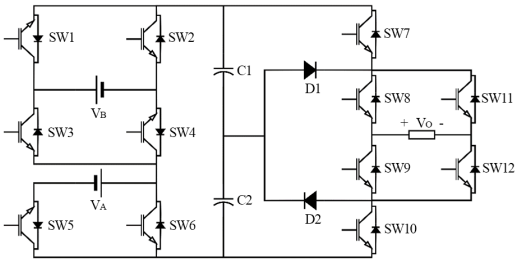

Figure 1. Proposed topology

Assume we have n number of voltage levels $L, L_0, L_1, L_2, \ldots, L_n$. The algorithm will calculate the distance D_n between adjacent levels for every ratio of V_B:V_A as follows:

$$\begin{aligned} D_1 &= L_1 - L_0 \\ D_2 &= L_2 - L_1 \\ D_n &= L_n - L_{n-1} \end{aligned} \tag{1}$$

To produce voltage levels that are equally spaced from each other as much as possible (to reduce the dv/dt stress and the THD.), the difference between the distances should ideally equal zero, but since the levels are asymmetrical this is not possible; Therefore, the algorithm iterates through Equation (2), and it outputs the best ratio.

$$D_2 - D_1 = D_3 - D_2 \cdots D_n - D_{n-1} = 0 \tag{2}$$

The design can be divided into two sections as shown in Figure 2.

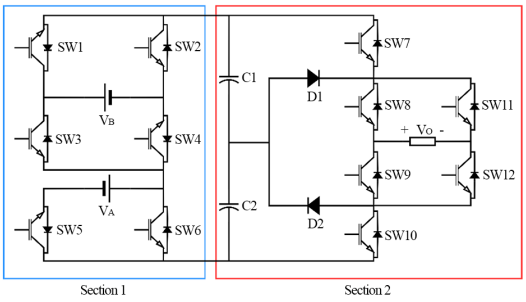

Figure 2. The two main sections of the system

The first section consists of SW1-6, and it is a modified version of a design proposed by [15], this circuit can generate four voltage levels, namely: V_A, V_B, $V_A + V_B$, $V_A - V_B$. The second section is a modified diode clamped inverter introduced in [12], which can divide the voltage by a factor of two, so the output of this section will be the voltage levels from section one divided by two: $V_A/2$, $V_B/2$, $(V_A + V_B)/2$, $(V_A - V_B)/2$. Switches SW11 and SW12 can provide a path to switch the output between section one and the diode clamped circuit. Also, switches SW8, SW9, SW11 and SW12 act like an H-Bridge and provide inversion for the output voltage.

2.2 *Modes of operation*

The states of the switches are shown in Table 1, where (0) indicates that the switch is off, (1) indicates it is on and an (×) means the state can be on or off as it does not affect the output voltage. Modes 1–8 are the positive half cycle, mode nine is the zero level and Modes 10–17 are the negative half cycle.

Table 1. Switching sequence for the proposed design

		Switches state											
Modes	Vo	SW1	SW2	SW3	SW4	SW5	SW6	SW7	SW8	SW9	SW10	SW11	SW12
1	$V_B/2$	1	0	0	1	0	1	1	1	0	0	0	1
2	V_B	1	0	0	1	0	1	1	1	0	1	0	1
3	$(V_A - V_B)/2$	0	1	1	0	1	0	1	1	0	0	0	1
4	$V_A/2$	0	1	0	1	1	0	1	1	0	0	0	1
5	$(V_A + V_B)/2$	1	0	0	1	1	0	1	1	0	0	0	1
6	$V_A - V_B$	0	1	1	0	1	0	1	1	0	1	0	1
7	V_A	0	1	0	1	1	0	1	1	0	1	0	1
8	$V_A + V_B$	1	0	0	1	1	0	1	1	0	1	0	1
9	0	×	×	×	×	×	×	×	0	1	0	0	1
10	$-V_B/2$	1	0	0	1	0	1	0	0	1	1	1	0
11	$-V_B$	1	0	0	1	0	1	1	0	1	1	1	0
12	$-(V_A - V_B)/2$	0	1	1	0	1	0	0	0	1	1	1	0
13	$-V_A/2$	0	1	0	1	1	0	0	0	1	1	1	0
14	$-(V_A - V_B)/2$	1	0	0	1	1	0	0	0	1	1	1	0
15	$-(V_A - V_B)$	0	1	1	0	1	0	1	0	1	1	1	0
16	$-V_A$	0	1	0	1	1	0	1	0	1	1	1	0
17	$-(V_A + V_B)$	1	0	0	1	1	0	1	0	1	1	1	0

Figure 3 shows all the different configurations that produce the desired 17 voltage levels. The blue lines in section one represent the connections between the two voltage sources, whose output is the input to the DC bus capacitors in section two. In section two the red lines show the current path from the DC bus capacitors to the load.

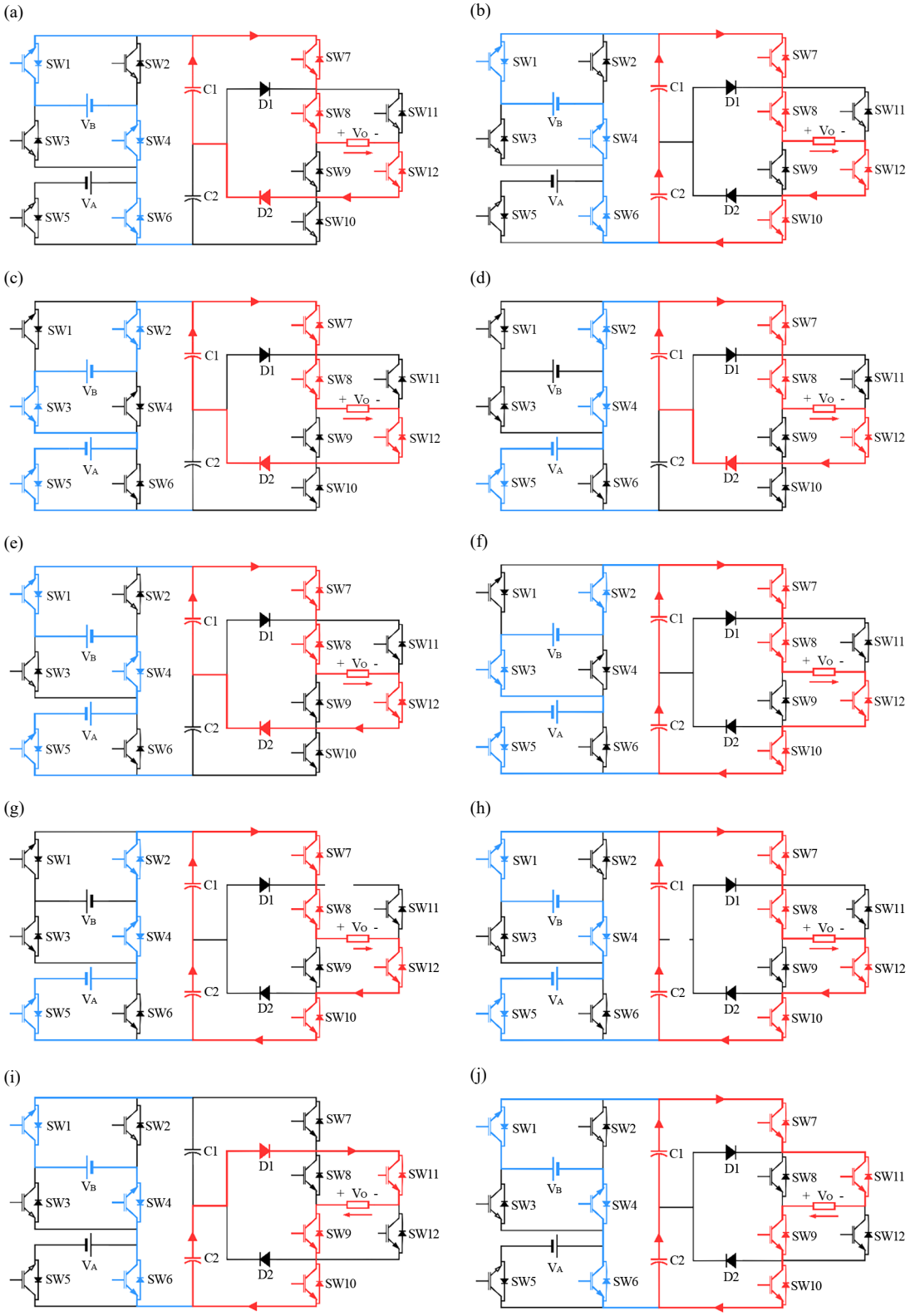
(a)
(b)
(c)
(d)
(e)
(f)
(g)
(h)
(i)
(j)
SW1
SW2
SW3
SW4
SW5
SW6
SW7
SW8
SW9
SW10
SW11
SW12
C1
C2
D1
D2
VB
VA
+ Vo -

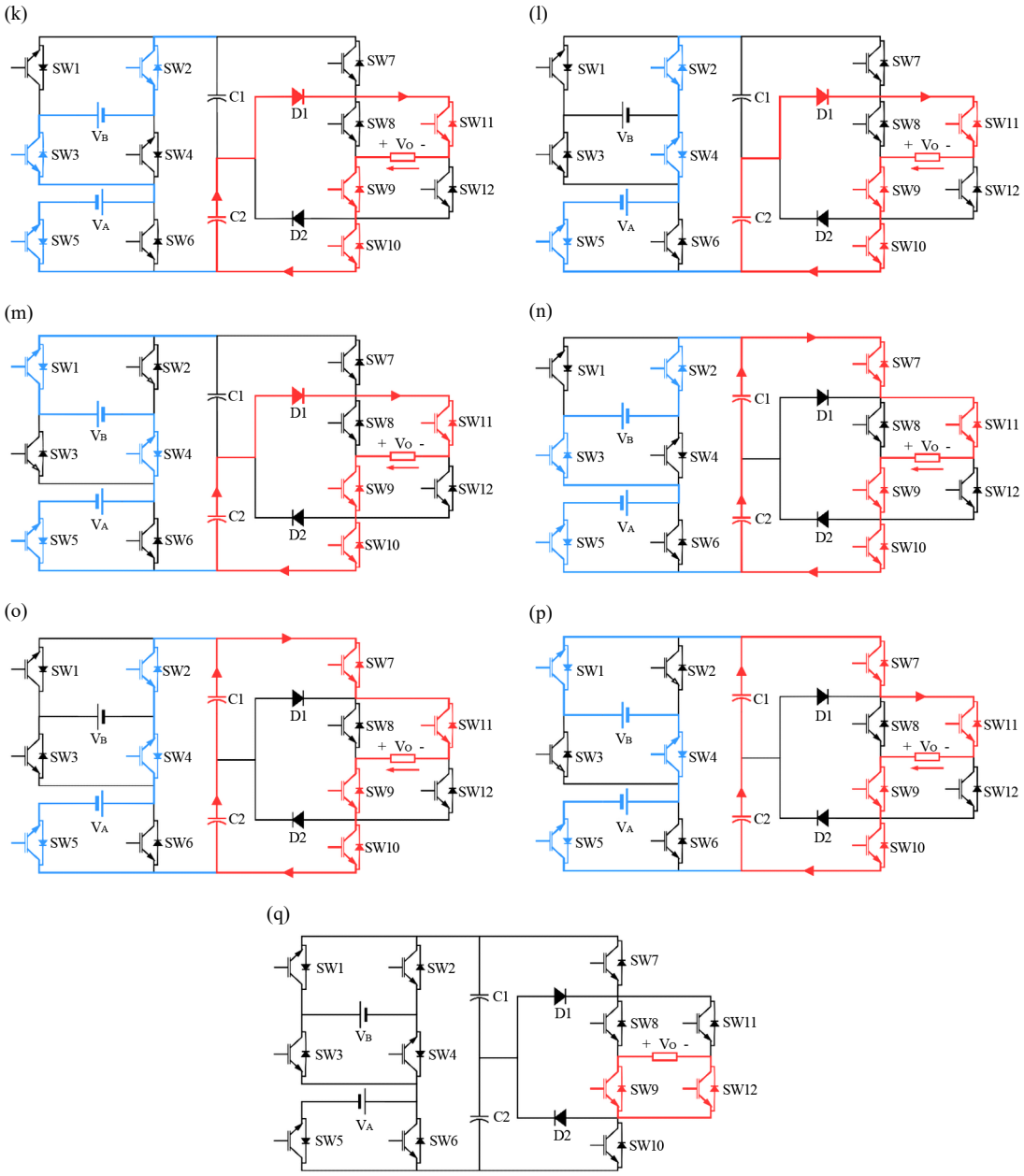

Figure 3. Modes of Operation. (a) $V_B/2$, (b) V_B, (c) $(V_A - V_B)/2$, (d) $V_A/2$, (e) $(V_A + V_B)/2$, (f) $V_A - V_B$, (g) V_A, (h) $V_A + V_B$, (i) $-V_B/2$, (j) $-V_B$, (k) $-(V_A - V_B)/2$, (l) $-V_A/2$, (m) $-(V_A + V_B)/2$, (n) $-(V_A - V_B)$, (o) $-V_A$, (p) $-(V_A + V_B)$, (q) Zero

2.3 *Control method*

Nearest Level Control (NLC) is a fundamental frequency switching technique used to control the inverter at a switching frequency of 50 Hz; Since the voltage levels are asymmetrical using this method simplifies the implementation, because the generated voltage levels can be outputted directly [16, 17]. The output voltage at a given moment is determined by checking what is the nearest voltage level at that moment relative to a reference waveform [18, 19].

Figure 4 shows the stepped waveform and the corresponding voltage levels for a 50 Hz sinewave reference.

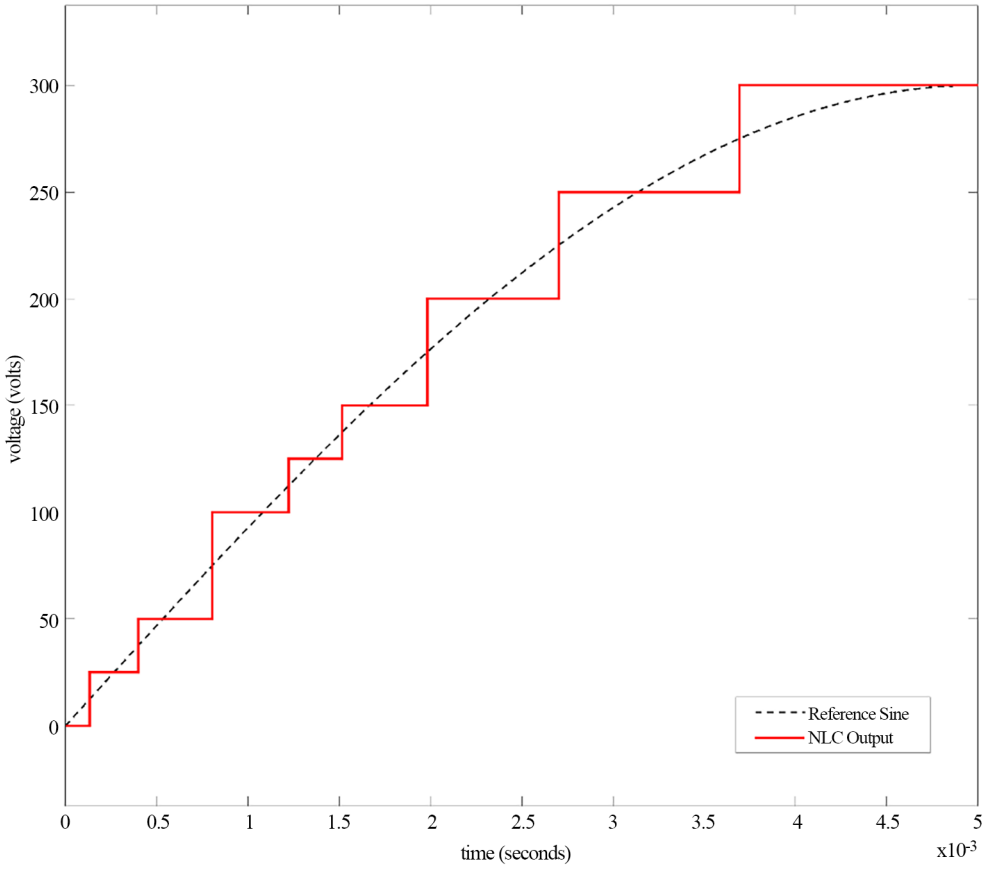

Figure 4. Nearest level control

3. Results and discussion

MATLAB/Simulink software was used to simulate the proposed design at a fundamental frequency of 50 Hz, values for the DC sources are V_A = 250 volts and V_B = 250 volts and $C_1 = C_2$ = 4700 µF. The switching pulses were generated using NLC. Figure 5 shows the control signals. Figure 6 shows the SIMULINK Model.

The design was evaluated for various loads, Figure 7a shows the output voltage for a 10 Ω resistive load, and it matches the expected results. The voltage THD is 5.67% as shown in Figure 7b.

An inductive load of 3.5 mH + 10 Ω was applied, giving a voltage THD of 5.82% and a current THD of 2.04% as shown in Figure 8a–d. It can be noticed that the voltage THD increased slightly due to distortion added by the inductive load.

For large inductances (larger than 10 mH), the distortion increases as shown in Figure 9 where a 40 mh + 20 Ω load was applied. The cause of this problem is the lack of a proper path for reverse inductor current at times when voltage is divided by two (i.e., Modes 1, 3, 4, 5, 10, 12, 13, 14), which causes these levels to be bypassed and the output behaves like Section 1.

This can be solved by replacing D1 and D2 with two switches, SW13 and SW14 respectively as shown in Figure 10, thus providing a controlled reverse current path if an inductive load with large inductance is applied. Control signals for SW13 and SW14 are shown in Figure 11 below.

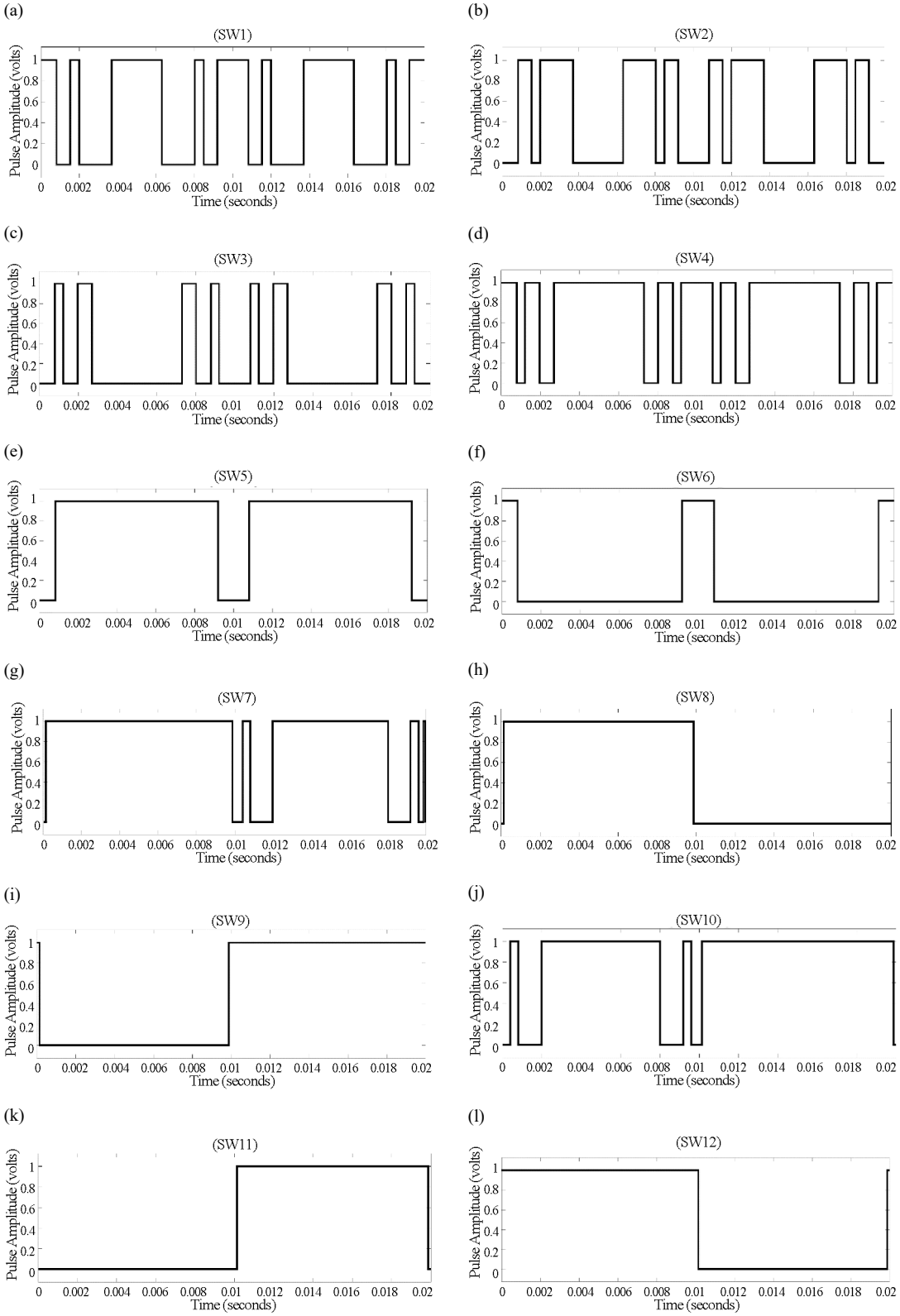

Figure 5. Control signals

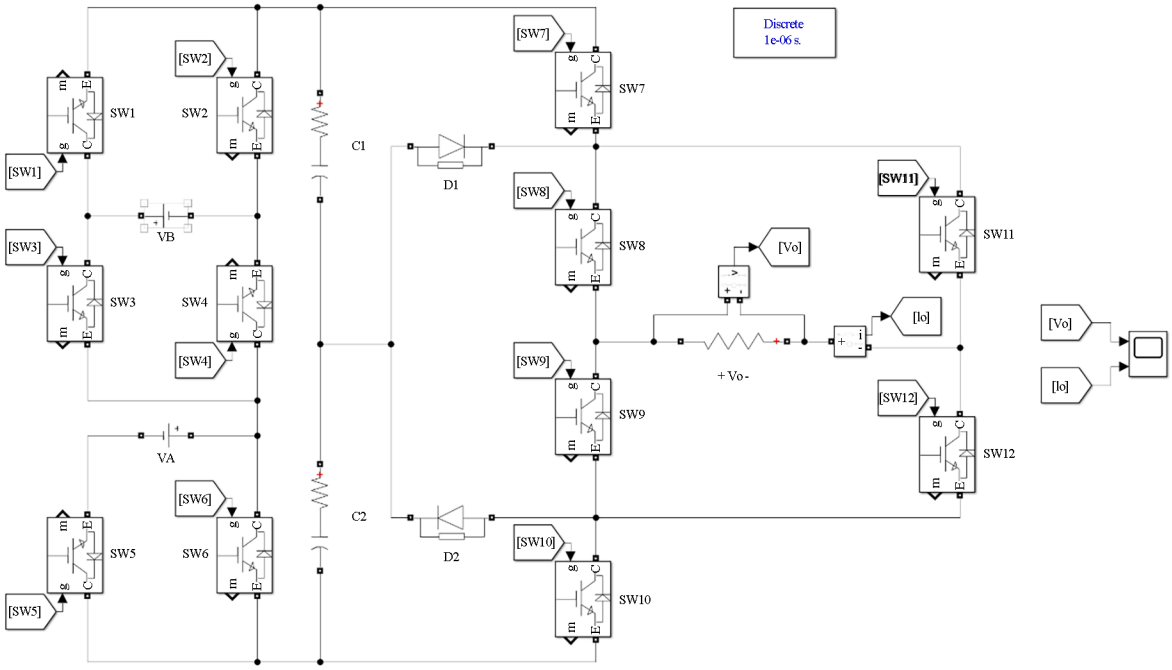

Figure 6. Simulink model

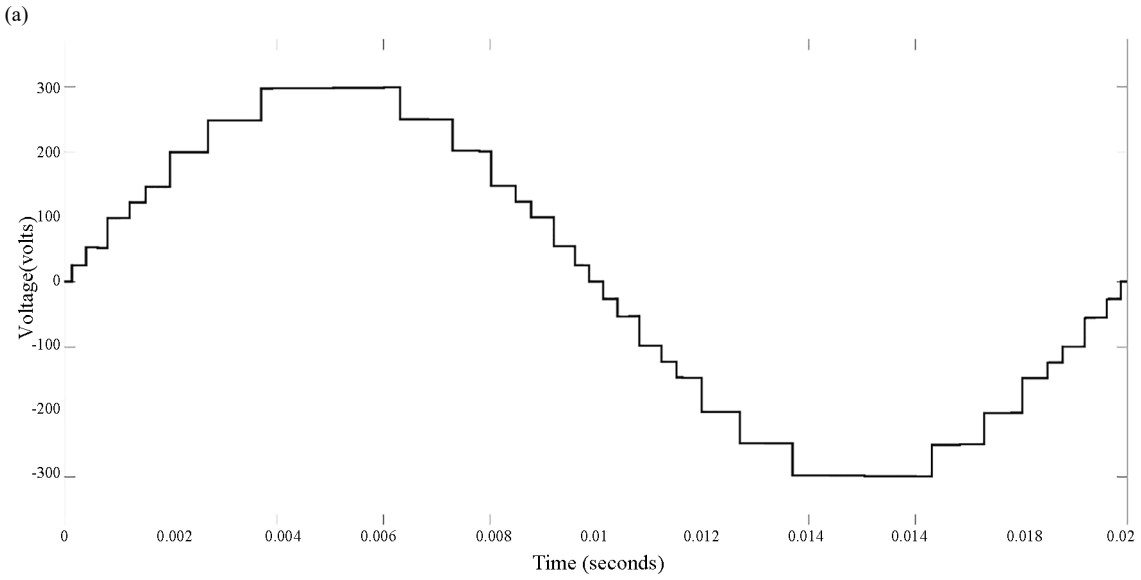

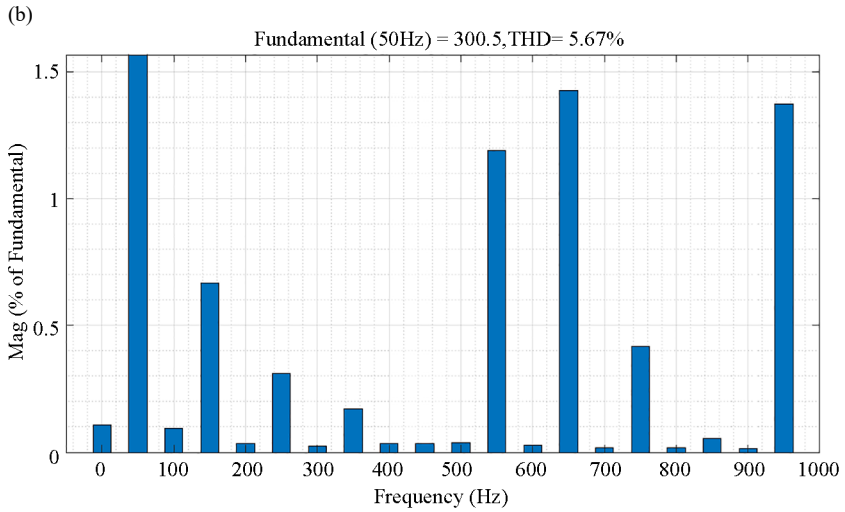

Figure 7. 10 Ω Resistive Load. (a) Output Voltage (b) Voltage THD

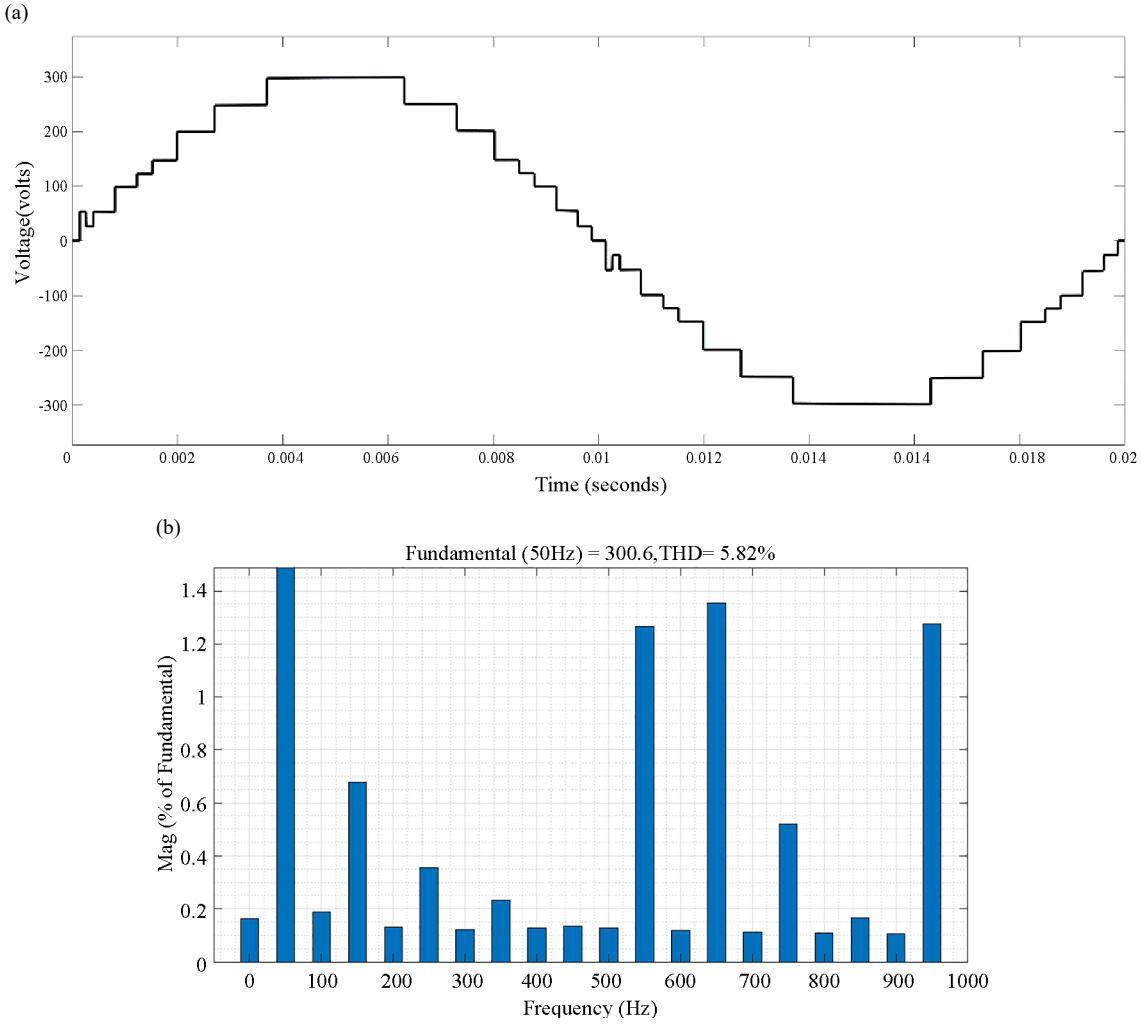

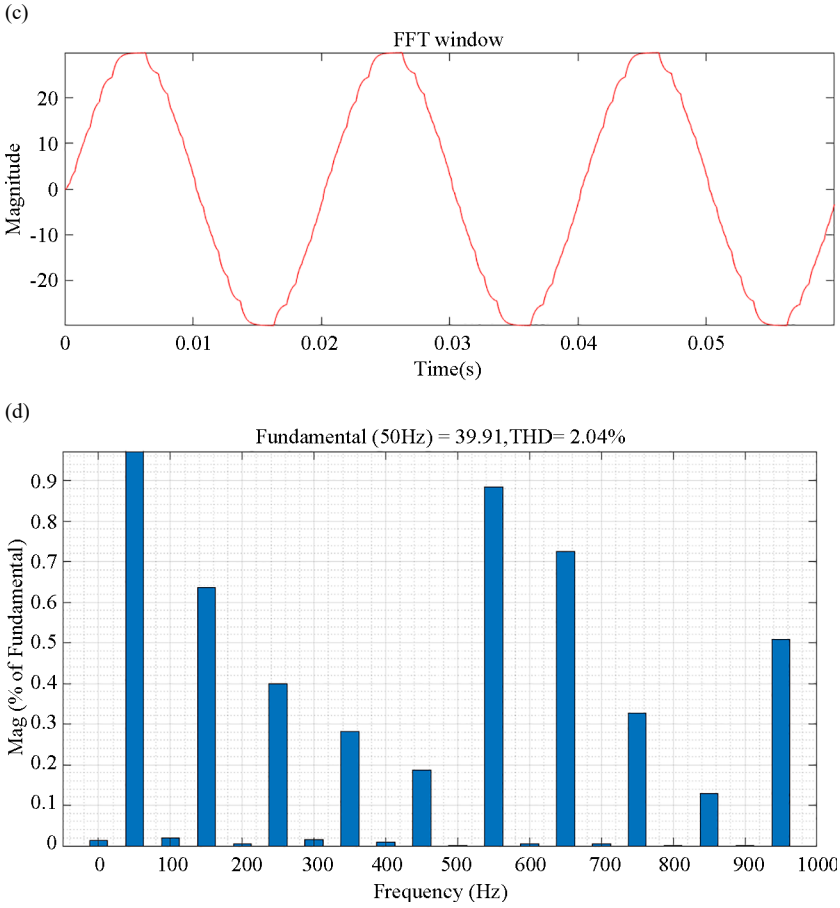

Figure 8. 3.5 mH + 10 Ω Inductive Load. (a) Output voltage (b) Voltage THD (c) Output current (d) Current THD

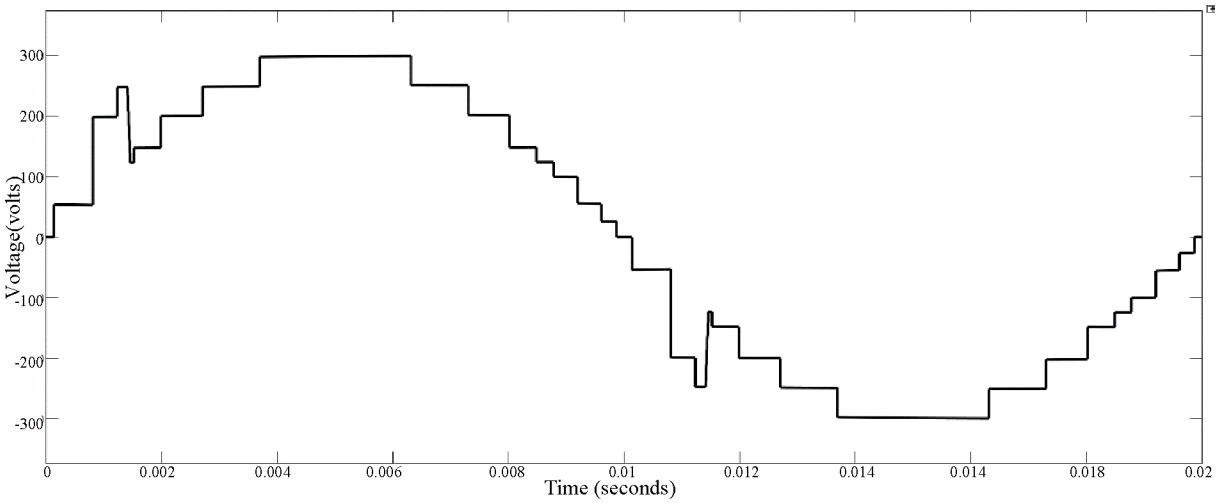

Figure 9. Output voltage for a 40 mH + 20 Ω Load

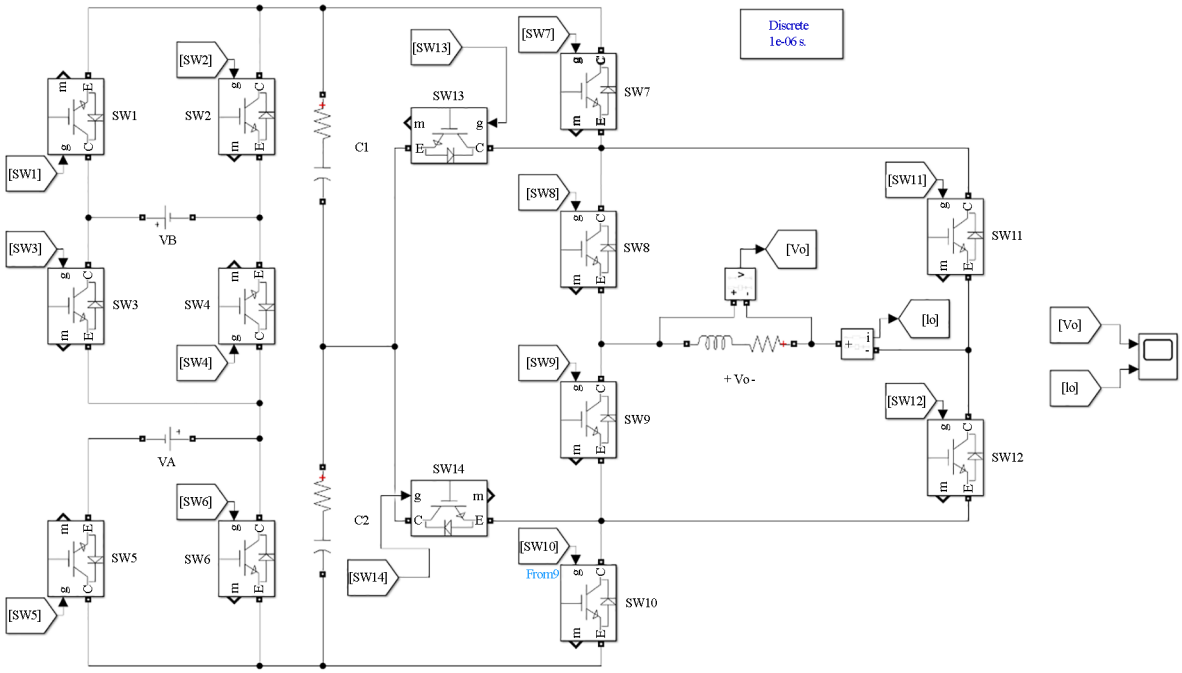

Figure 10. Modified circuit

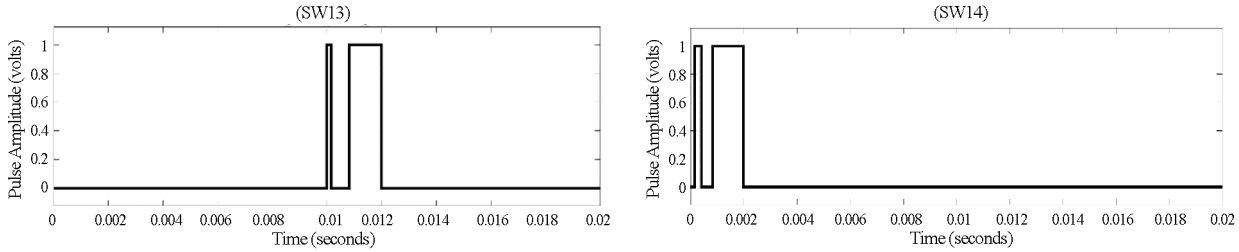

Figure 11. Control signals for switches SW13 and SW14

Figure 12a shows output voltage of the modified circuit for the same 40 mh + 20 Ω load, it exhibits a voltage THD of 5.86% and a current THD of 0.68% as shown in Figure 13b.

The modified circuit has been tested under a sudden input change as shown in Figure 14, where VA dropped from 250 volts to 210 volts, and VB dropped from 50 volts to 40 volts.

Figure 15 shows a sudden load change condition, where the load changed from 25 mh + 7 Ω to 40 mh + 15 Ω.

Two main power loss mechanisms affect switching devices, conduction losses and switching losses; Switching losses are prominent in topologies with high switching frequency, while conduction losses are more dominant in low switching frequency designs. Since NLC is a low switching frequency technique, switching losses can be neglected.

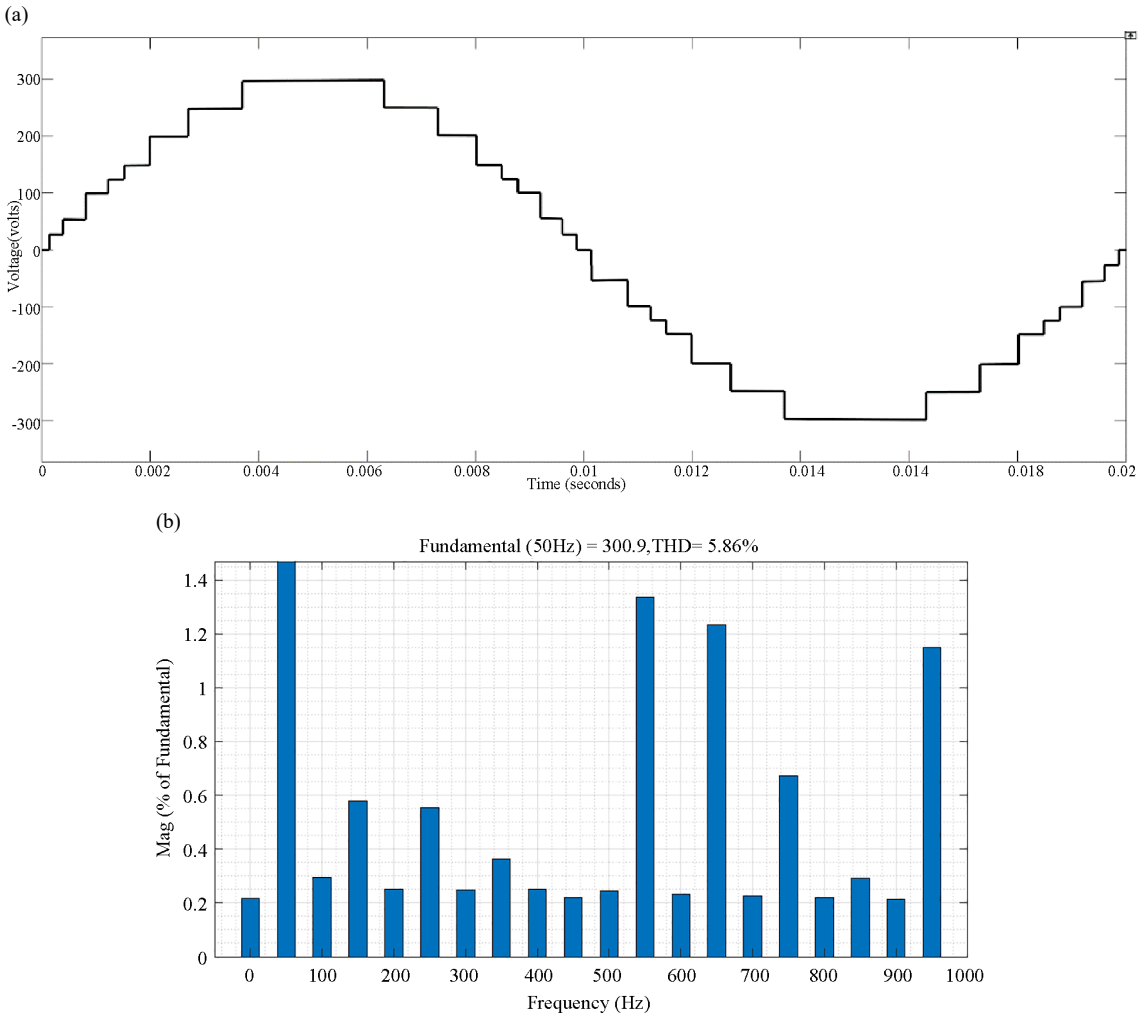

Figure 12. Modified circuit output for 40 mH + 20 Ω inductive load. (a) Output voltage (b) voltage THD

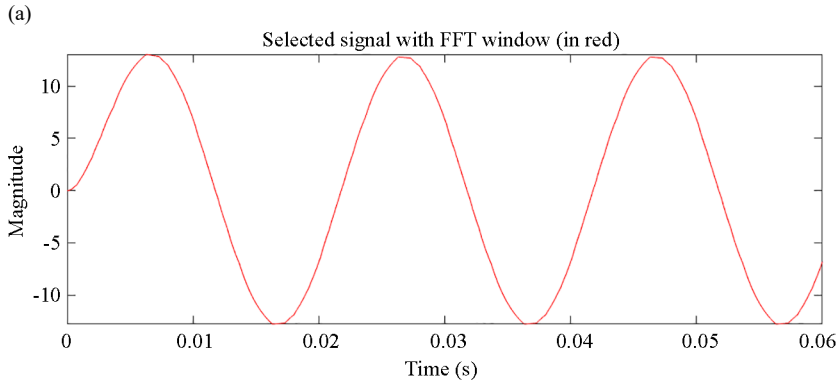

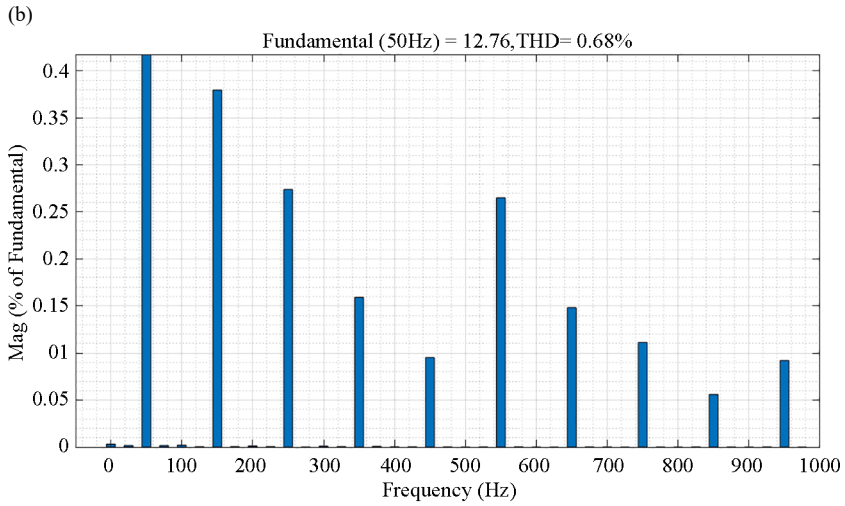

Figure 13. Modified circuit output for 40 mH + 20 Ω inductive load. (a) Output current (b) current THD

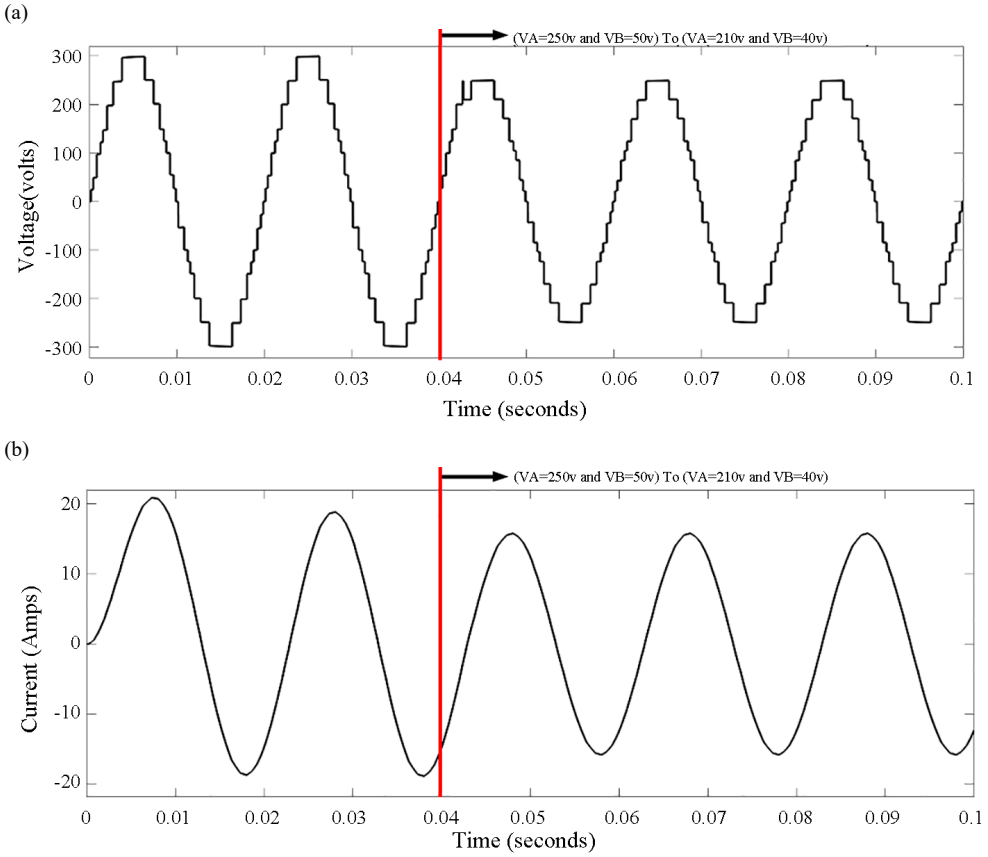

Figure 14. Sudden input change. (a) Output voltage (b) output current

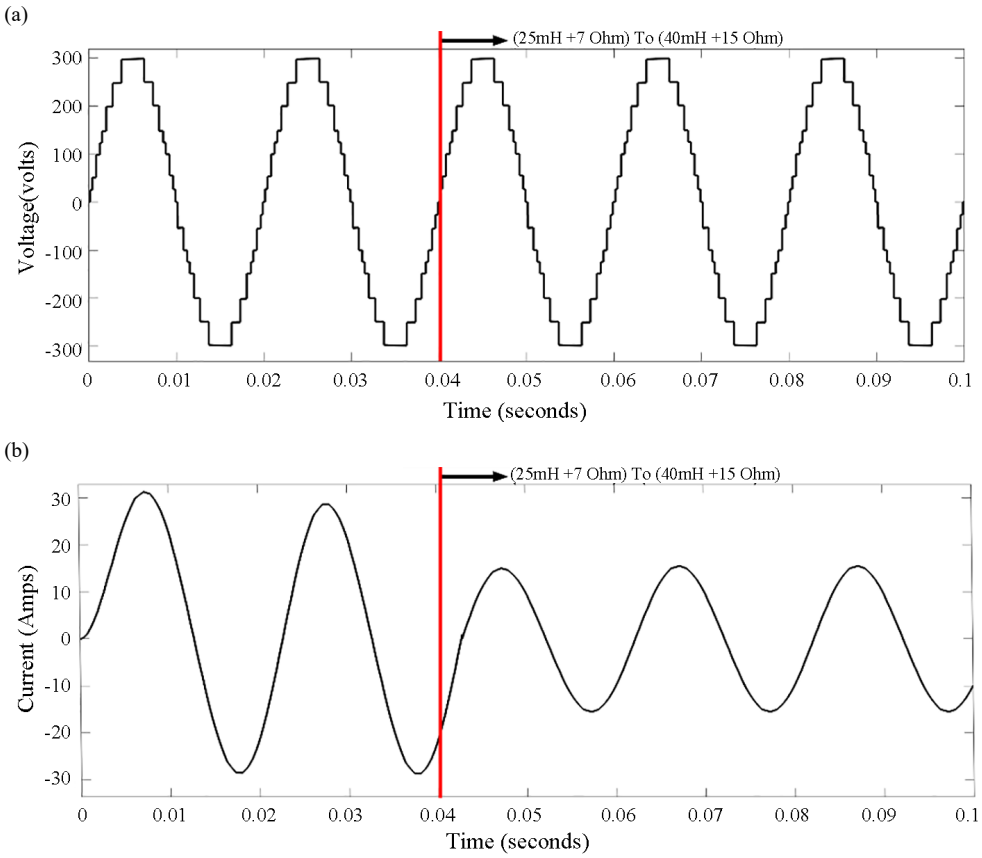

Figure 15. Sudden load change. (a) Output voltage (b) output current

Conduction losses are caused by the on-resistance of the switch R_S and the anti-parallel diode R_D. The conduction losses of the switch P_{CS} and of the diode P_{CD} can be calculated as follows [16]:

$$P_{CD} = V_S i(t) + \left[R_S i^{\beta}(t)\right] i(t) \tag{3}$$

$$P_{CD} = V_D i(t) + R_D i^2(t) \tag{4}$$

where V_S is the switch voltage, V_D is the diode voltage and β is a data-sheet constant. The average conduction power loss during a period of time P_C, can be calculated using Equation (5) as follows:

$$P_C = \frac{1}{\pi}\int_0^{\pi} [N_S(t)P_{CS}(t) + N_D(t)P_{CD}(t)]\,dt \tag{5}$$

where N_S is the number of switches and N_D is the number of diodes conducing at the time instant t.

The efficiency of the inverter η_{inv} can be found using Equation (6):

$$\eta_{inv} = \frac{P_{AC}}{P_{DC}} \tag{6}$$

where P_{AC} is the output AC power, and P_{DC} is the input DC power. The efficiency in the resistive load case is 92.11%.

Different 17-level inverters are compared in terms of the number of components in Table 2.

Table 2. Comparison of various 17-level topologies

Feature	[13]	[20]	[21]	Proposed (modified)	Proposed
Switching devices	11	16	20	14	12
DC sources	3	4	1	2	2
Capacitors	0	4	4	2	2
Diodes	0	0	2	0	2

Figure 16a shows the output voltage of the design introduced in [13] that uses 11 switches, which is the lowest number of switches in this comparison, but it needs 3 independent voltage sources to operate, this puts it at a disadvantage especially in terms of size. In [20] a CHB-MLI design is introduced, with a total switch count of 16, and four voltage sources and four DC bus capacitors. In one hand, the levels are symmetrical, and the output voltage shown in Figure 16b has a THD of 4.12%, on the other hand, the number of sources, switches and capacitors increases the size and the cost of the inverter dramatically. [21] presented a design utilizing only one voltage source. However, 20 switches are required, in addition to 4 capacitors and two diodes. The output voltage is shown in Figure 16c. Even though one source is needed, the number of switches is the highest among all the compared topologies, and it contributes to a noticeable increase in the cost.

(a)

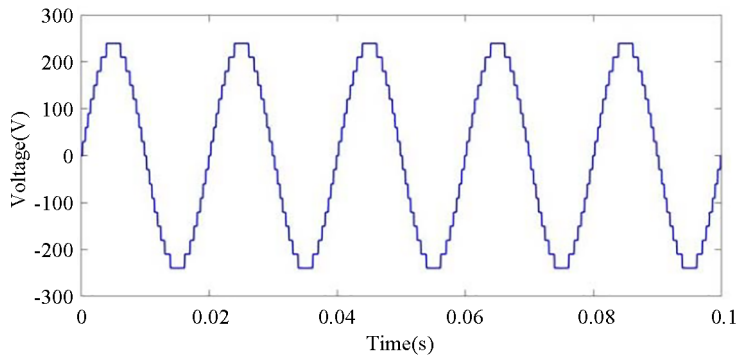

(b)

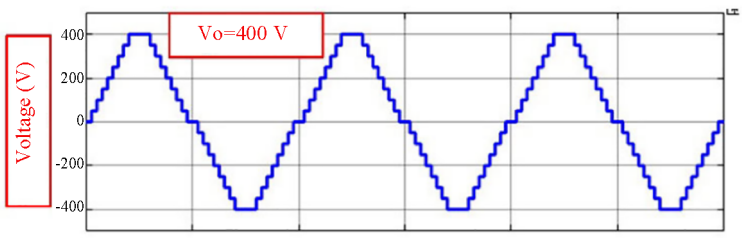

(c)

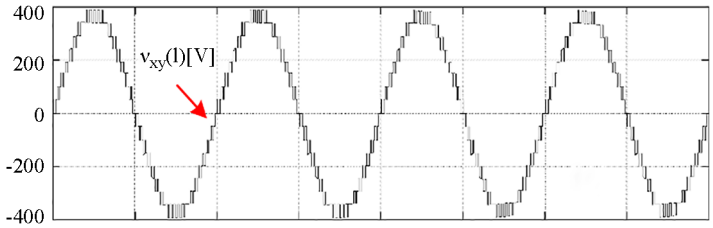

Figure 16. Output voltage of (a) reference [13]. (b) reference [20]. (c) reference [21]

It can be noticed that the proposed designs achieve a balance between the number of switches, DC sources and capacitors. Thus, making it a good candidate for many use cases, without being very bulky or very expensive.

4. Conclusions

In this paper a novel promising multilevel inverter was introduced. The number of components and DC supplies was reduced while keeping a high number of output voltage steps and reasonable THD, the main approach to do that was by combining a DC voltage summing and subtracting circuit with a circuit that divides the DC voltage by two.

An algorithm was written to design an iteration method that gives the best ratio between the two input DC supplies.

Two circuits were designed, both generating 17-levels from two DC sources and two DC bus capacitors; The first one is suitable for resistive loads or low inductance loads (below 10 mH), it employs only 12 switching devices. The second circuit (the all-loads circuit) solves a problem related to loads with large inductance by adding two more switches with a total switch count of 14. Both circuits showed good current THD without any filtering or modulation.

Acknowledgment

We would like to thank Yarmouk University for all of its support and encouragement while working on this research.

Conflict of interest

There is no conflict of interest for this study.

References

[1] S. R. Khasim and C. Dhanamjayulu, “Design and implementation of asymmetrical multilevel inverter with reduced components and low voltage stress,” *IEEE Access*, vol. 10, pp. 3495-3511, 2022. https://doi.org/10.1109/access.2022.3140354.

[2] Z. E. Abdulhamed, A. H. Esuri, and N. A. Abodhir, “New topology of asymmetrical nine-level cascaded hybrid bridge multilevel inverter,” In Proc. 2021 IEEE 1st International Maghreb Meeting of the Conference on Sciences and Techniques of Automation Control and Computer Engineering MI-STA, Tripoli, Libya, May 25-27, 2021. https://doi.org/10.1109/MI-STA52233.2021.9464511.

[3] P. Omer, J. Kumar, and B. S. Surjan, “A review on reduced switch count multilevel inverter topologies,” *IEEE Access*, vol. 8, pp. 22281-22302, 2020. https://doi.org/10.1109/access.2020.2969551.

[4] X. Zhang, T. Zhao, W. Mao, D. Tan, and L. Chang, "Multilevel inverters for grid-connected photovoltaic applications: examining emerging trends," *IEEE Power Electronics Magazine*, vol. 5, no. 4, pp. 32-41, 2018. https://doi.org/10.1109/mpel.2018.2874509.

[5] A. Poorfakhraei, M. Narimani, and A. Emadi, "A review of multilevel inverter topologies in electric vehicles: current status and future trends," *IEEE Open Journal of Power Electronics*, vol. 2, pp. 155-170, 2021. https://doi.org/10.1109/ojpel.2021.3063550.

[6] L. K. Haw, N. A. Jefry, and W. K. Ing, "The new hybrid multilevel inverter with reduced number of switches," In Proc. 2021 IEEE 11th International Conference on System Engineering and Technology (ICSET), Shah Alam, Malaysia, Nov. 6, 2021. https://doi.org/10.1109/ICSET53708.2021.9612532.

[7] G. K. Srinivasan, M. Rivera, V. Loganathan, D. Ravikumar, and B. Mohan, "Trends and challenges in multi-level inverter with reduced switches," *Electronics*, vol. 10, no. 4, 2021. https://doi.org/10.3390/electronics10040368.

[8] M. O. Alsumady, Y. K. Alturk, A. Dagamseh, and M. Tantawi, "Controlling of DC-DC buck converters using microcontrollers," *International Journal of Circuits Systems and Signal Processing*, vol. 15, pp. 197-202, 2021. https://doi.org/10.46300/9106.2021.15.22.

[9] S. S. Barah and S. Behera, "An optimize configuration of H-bridge multilevel inverter," In Proc. 2021 1st International Conference on Power Electronics and Energy (ICPEE), Bhubaneswar, India, Jan. 2-3, 2021. https://doi.org/10.1109/ICPEE50452.2021.9358533.

[10] A. Y. Mirza, H. Nyugen, A. M. Bazzi, and Y. Cao, "Investigating the effect of multilevel inverters on motor stator insulation stress," In Proc. 2021 IEEE Energy Conversion Congress and Exposition (ECCE), Vancouver, BC, Canada, Oct. 10-14, 2021, pp. 5569-5572. https://doi.org/10.1109/ecce47101.2021.9595285.

[11] J.-S. Choi and F.-S. Kang, "Seven-level PWM inverter employing series-connected capacitors paralleled to a single DC voltage source," *IEEE Transactions on Industrial Electronics*, vol. 62, no. 6, pp. 3448-3459, 2015. https://doi.org/10.1109/TIE.2014.2370948.

[12] A. Kahwa, H. Obara, and Y. Fujimoto, "Design of 5-level reduced switches count H-bridge multilevel inverter," In Proc. 2018 IEEE 15th International Workshop on Advanced Motion Control (AMC), Tokyo, Japan, Mar. 9-11, 2018. https://doi.org/10.1109/AMC.2019.8371060.

[13] K. S. and M. Das B, "A low switching frequency based 17 level inverter with nearest level control," In Proc. 2020 IEEE International Conference on Power Electronics, Drives and Energy Systems (PEDES), Jaipur, India, Dec. 16-19, 2020, pp. 1-5. https://doi.org/10.1109/pedes49360.2020.9379461.

[14] M. Pandey, V. B. Borghate, K. M. Gajbhiye, S. Sabyasachi, and H. B. Gobburi, "Design and development of multilevel inverter topology," In Proc. 2020 IEEE 1st International Conference on Smart Technologies for Power, Energy and Control (STPEC), Nagpur, India, Sep. 25-26, 2020. https://doi.org/10.1109/STPEC49749.2020.9297663.

[15] M. N. A. Ghamudi, Z. E. Abdulhamed, and A. H. Esuri, "A modified topology of asymmetrical 9-levels cascaded multilevel inverter," In Proc. 2021 IEEE 1st International Maghreb Meeting of the Conference on Sciences and Techniques of Automation Control and Computer Engineering MI-STA, Tripoli, Libya, May 25-27, 2021. https://doi.org/10.1109/MI-STA52233.2021.9464358.

[16] M. S. Bin Arif, U. Mustafa, S. B. M. Ayob, J. Rodriguez, A. Nadeem, and M. Abdelrahem, "Asymmetrical 17-level inverter topology with reduced total standing voltage and device count," *IEEE Access*, vol. 9, pp. 69710-69723, 2021. https://doi.org/10.1109/access.2021.3077968.

[17] S. Kouro, R. Bernal, H. Miranda, C. A. Silva, and J. Rodriguez, "High performance torque and flux control for multilevel inverter fed induction motors," *IEEE Transactions on Power Electronics*, vol. 22, no. 6, pp. 2116-2123, 2007. https://doi.org/10.1109/TPEL.2007.909189.

[18] A. R. Kumar, T. Deepa, S. Padmanaban, and D. P. Kothari, "A guide to nearest level modulation and selective harmonics elimination modulation scheme for multilevel inverters," In Proc. 2019 Innovation in Power and Advanced Computing Technologies (i-PACT), Vellore, India, Mar. 22-23, 2019, pp. 1-8. https://doi.org/10.1109/i-pact44901.2019.8960205.

[19] P. M. Meshram and V. B. Borghate, "A simplified nearest level control (NLC) voltage balancing method for modular multilevel converter (MMC)," *IEEE Transactions on Power Electronics*, vol. 30, no. 1, pp. 450-462, 2014. https://doi.org/10.1109/tpel.2014.2317705.

[20] C. Dhanamjayulu, D. Prasad, S. Padmanaban, P. K. Maroti, J. B. Holm-Nielsen, and F. Blaabjerg, "Design and implementation of seventeen level inverter with reduced components," *IEEE Access*, vol. 9, pp. 16746-16760, 2021. https://doi.org/10.1109/access.2021.3054001.

[21] D. K. Patel, V. P. Pal, K. Baitha, and D. Kumar, “A novel 17-level switched-capacitor multilevel inverter with reduced device count,” In Proc. 2022 2nd International Conference on Emerging Frontiers in Electrical and Electronic Technology (ICEFEET), Patna, India, Jun. 24-25, 2022. https://doi.org/10.1109/ICEFEET51821.2022.9847689.